



Effects of rare earth Ce addition on microstructure and mechanical properties of impure copper containing Pb

Hai-hong LI¹, Xiao LIU¹, Yang LI¹, Shi-hong ZHANG², Yan CHEN², Song-wei WANG², Jin-song LIU², Jin-hu WU³

1. College of Nuclear Equipment and Nuclear Engineering, Yantai University, Yantai 264005, China;

2. Institute of Metal Research, Chinese Academy of Sciences, Shenyang 110016, China;

3. College of Metallurgy and Energy, North China University of Science and Technology, Tangshan 063210, China

Received 2 September 2019; accepted 12 April 2020

Abstract: The effects of rare earth Ce on the microstructure and mechanical properties of impure copper containing Pb were investigated using OM, SEM, EPMA, TEM and tensile testing. TEM and EDS analysis reveal that spherical CePb₃ particles form after Ce addition. CePb₃ particles, with average size of ~3.6 μm, homogeneously distribute in the Cu matrix. Due to small lattice misfit (~4.62%) with Cu matrix, CePb₃ particles can act as effective nucleation sites beneficial to the grain refinement. Pb at grain boundaries seriously deteriorates the mechanical properties of Cu. The tensile strength and the elongation of Cu–0.1Pb are decreased by 43.1% and 56.7% compared with those of pure copper, respectively. Ce can purify grain boundaries, cause the precipitation of CePb₃ particles and refine grain sizes, which contribute to significant improvement of the mechanical properties of Cu. Compared with Cu–0.1Pb, the tensile strength (179 MPa) and the elongation (38.5%) of Cu–0.1Pb–0.3Ce are increased by 117.6% and 151.6%, respectively.

Key words: Ce addition; impure copper containing Pb; CePb₃ second phase particle; lattice misfit; grain refinement; mechanical property

1 Introduction

With the rapid development of copper processing industry worldwide, the shortage of raw copper materials is becoming increasingly critical [1,2]. High efficient and reasonable utilization of impure copper plays a vital role in addressing the scarcity of copper resources [3–5]. However, the mechanical properties and the processability of copper products are deteriorated due to the existence of impurity elements, which limits the application of impure copper [6–8]. Pb, as a beneficial alloying element, can improve the wear and corrosion resistance of copper alloys. Pb is a fairly common impure element in copper

recycling. Due to the low solubility of Pb in Cu and a lower melting point than that of Cu, Pb in impure copper mainly distributes on grain boundary, resulting in the decreasing of the binding forces of grain boundaries [9] and the worsening of mechanical properties.

Rare earth (RE) elements present active chemical properties and can react with the impurities in copper by forming RE-rich compounds with high melting points [10–13]. Therefore, RE can change the existence forms of the impurities in copper and improve the properties of copper remarkably. LIN et al [14] found that RE addition decreased the contents of O, Pb, Bi and Sn in impure copper due to the formation of RE-rich compounds with low densities and high melting

Foundation item: Projects (ZR2018MEE005, ZR2018MEE016) supported by the Natural Science Foundation of Shandong Province, China; Project (J18KA059) supported by the Higher Educational Science and Technology Program of Shandong Province, China; Project (HJ16B01) supported by the Doctoral Fund of Yantai University, China

Corresponding author: Hai-hong LI; Tel/Fax: +86-535-6903650; E-mail: hhli@ytu.edu.cn

DOI: 10.1016/S1003-6326(20)65320-1

points. DUAN et al [15] also reported that Ce reduced the contents of the impurities in impure copper and improved the elongation of copper lines. CHEN et al [16] and ZHANG et al [17] revealed that RE removed the impurities in copper and refined the grain size. LI et al [18] stated that rare earth Ce could prevent the segregation of Pb in high-lead bronze by forming some Ce-rich compounds. Also, due to the strengthening and grain refinement effects, RE-rich second phases can also improve the tensile properties and tribological properties of copper alloys [19,20]. It should be mentioned that most of the previous studies were focused on the influence of RE on pure copper and copper alloys. However, the role of RE with a single impurity (Pb) is still unclear so far [21,22]. Especially, the distribution of RE-rich compounds and the refinement mechanism are poorly understood. As one of important light RE elements, Ce has very active chemical properties [23,24]. Here, the effects of Ce on microstructures and mechanical properties of impure copper containing 0.1 wt.% Pb are investigated, and the actions between Ce and Pb are also discussed. The obtained results in this research may provide a theoretical basis for the direct reuse of impure copper.

2 Experimental

In order to reduce the interference of other elements, raw materials of electrolytic copper with a purity of 99.97 wt.%, pure Ce with a purity of 99 wt.% and pure Pb with a purity of 99.99 wt.% were employed. Electrolytic copper was first melted completely in a graphite crucible by a vacuum induction furnace under an argon atmosphere. And then, pure Pb wrapped by pure copper foils was added into the copper melt at 1180 °C. After cooling, the impure copper ingot containing Pb was cut and melted secondly. Pure Ce wrapped by pure copper foils was added to the melt. The melt was stirred and isothermally held for 10 min to ensure that Ce was dissolved thoroughly. At

1180 °C, the melt was poured into an iron mould preheated to ~300 °C. The ingot was cooled to ~800 °C at a cooling rate of ~60 °C/s and then cooled to room temperature naturally.

The practical contents of Pb and Ce in copper were determined using an Optima 7300DV inductively coupled plasma-atomic emission spectrometry (ICP-AES). Chemical compositions of the alloys are listed in Table 1. Under vacuum circumstance, Ce still had a 10% burning loss for oxidation. Tensile tests were performed by an INSTRON 5582 electronic universal testing machine at an ambient temperature according to GB/T228B using sheet specimens, and the cross-head speed was 1 mm/min. The microstructures were observed by a ZMEF4A optical microscope (OM) before and after the etching in a solution of ferric nitrate (4 g) and water (100 mL). The grain size was measured by the intercept method using an image-pro plus software. The existence forms of Pb, the distribution of second phases and the fractography were examined by an SSX-550 scanning electron microscopy (SEM). The crystal structure of the second phases was characterized by a JEM-2100F transmission electron microscopy (TEM).

3 Results and discussion

3.1 Existence forms of Pb and Ce in copper

Figure 1 shows the microstructure and energy dispersive spectrum (EDS) of Cu-0.1Pb. As can be seen from Fig. 1(a), there are some small black particles on the grain boundaries of copper matrix. A large number of white particles exist on grain boundaries (Fig. 1(b)). These particles present short rod morphology at high magnification, and the length is ~2 μm, as shown in Fig. 1(c). EDS analysis verifies that the content of Pb in these particles is 89.1 wt.% (Fig. 1(d)).

Pb is an impurity element with a low melting point in copper. A small amount of Pb can agglomerate near the grain boundaries during the

Table 1 Chemical compositions of impure copper containing Pb before and after Ce addition (wt.%)

Sample	Pb addition	Ce addition	Practical content of Pb	Practical content of Ce	Cu
Pure copper	0	0	0	0	Bal.
Cu-0.1Pb	0.1	0	0.1	0	Bal.
Cu-0.1Pb-0.3Ce	0.1	0.3	0.1	0.27	Bal.

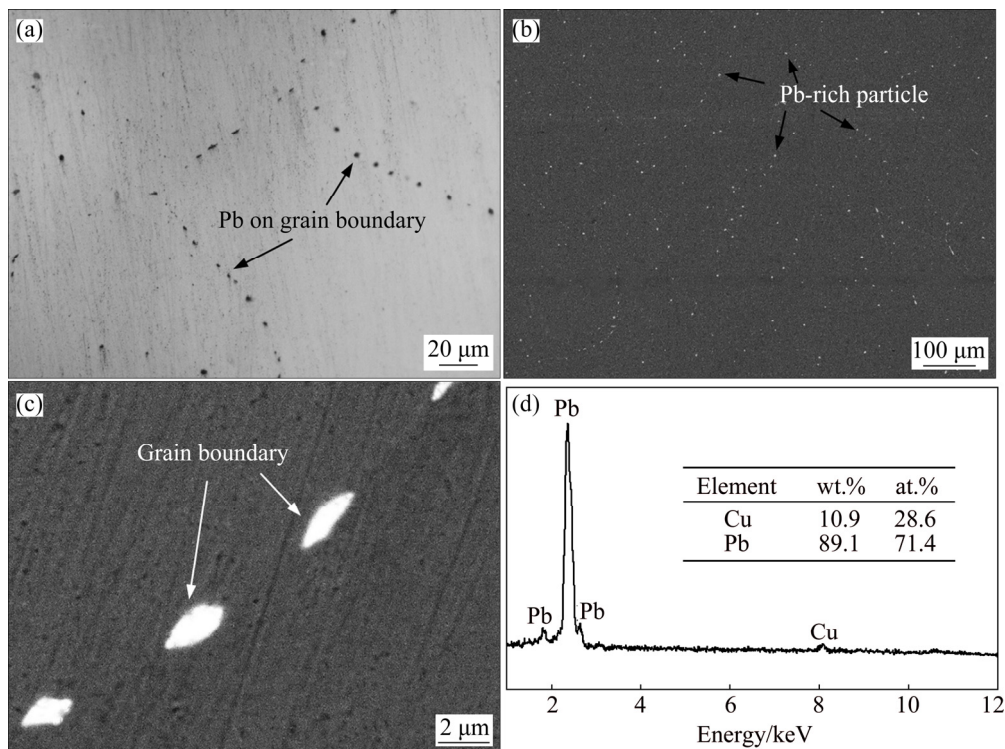


Fig. 1 Microstructure and EDS of Cu-0.1Pb: (a) OM; (b, c) BSE images; (d) EDS results of white precipitate on grain boundary in (c)

solidification process. According to Cu-Pb binary phase diagram [25], there is a eutectic transformation at 326 °C. Pb-rich phases grow along grain boundaries and gather at the grain boundaries finally, indicating the divorced eutectic structure. Furthermore, the equilibrium partition coefficient (k_0) of Pb in Cu is less than 1 [26]. Pb segregates between the liquid phase and the solid-liquid interface and solidifies on grain boundaries at last. The segregation of Pb element on grain boundaries can deteriorate the mechanical properties of copper seriously.

Figure 2 shows the microstructure and EDS of Cu-0.1Pb-0.3Ce. From Figs. 2(a, b), the number of small particles on grain boundaries decreases obviously after Ce addition. Many spherical second phase particles with a size of $\sim 3.6 \mu\text{m}$ are formed in the interior of the grains. The wettability of these particles and the copper matrix is poor, leading to formation of the spherical profile (Fig. 2(c)). These second phase particles are Ce, Pb compounds. The molar ratio of Pb to Ce is about 3:1 (Fig. 2(d)). Figure 3 shows the EPMA result of the second phase. From Fig. 3, it can be seen that elements of Ce and Pb distribute uniformly, and the content of Cu is low. Figure 4 shows the TEM image and

selected area electron diffraction pattern of the second phase. TEM combined with EDS analysis demonstrate that the structure of second phase particle is CePb_3 with AuCu_3 -type fcc structure and space group of $pm3m$. The structure parameter is $a=0.4876 \text{ nm}$ [27].

Ce addition changes the existence forms of Pb. Pb exists in the form of CePb_3 particles, which distribute homogeneously in Cu matrix instead of at grain boundary. Ce has very active chemical properties, and there are strong interactions between atoms of Ce and Pb. Therefore, Ce reacts with Pb rapidly, leading to the formation of CePb_3 . The melting point of CePb_3 is about 1170 °C, which is higher than that of Cu (1083 °C) [27]. CePb_3 solidifies before copper during the cooling process and exists in the interior of the grains.

3.2 Effects of Ce on microstructure of impure copper containing Pb

Figure 5 shows the optical micrographs of impure copper containing Pb before and after Ce addition. It is clear that pure copper has a large columnar structure, and the average columnar crystal spacing is $\sim 1092.2 \mu\text{m}$ (Fig. 5(a)). Addition of 0.1 wt.% Pb refines the columnar structure of

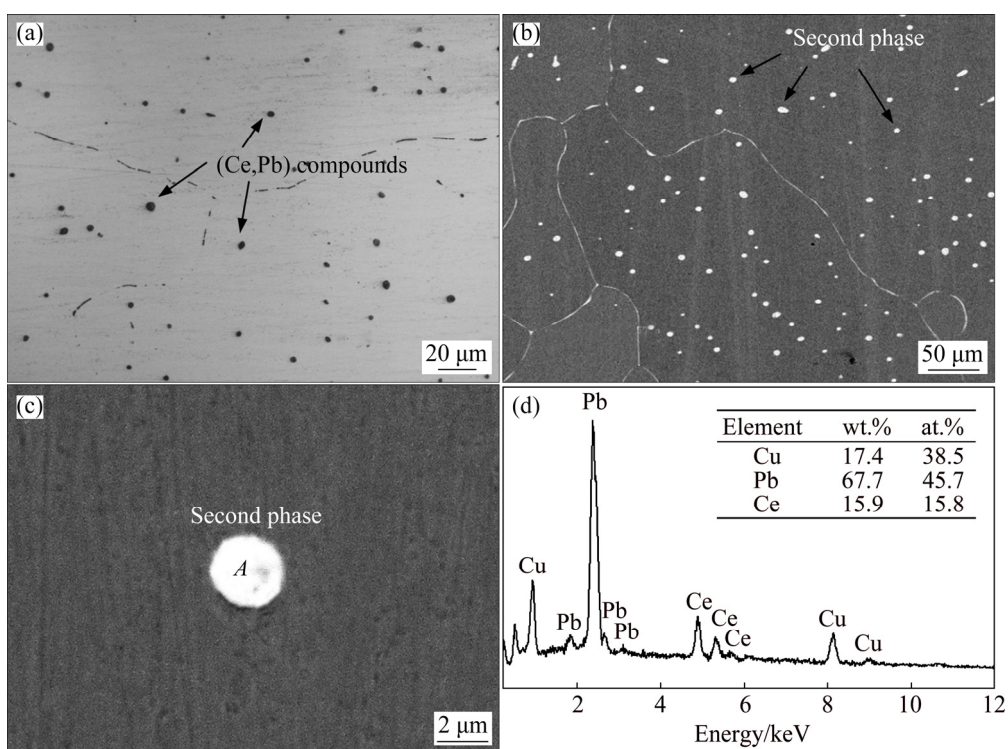


Fig. 2 Microstructure and EDS of Cu-0.1Pb-0.3Ce: (a) OM; (b, c) BSE images; (d) EDS results of Point A in (c)

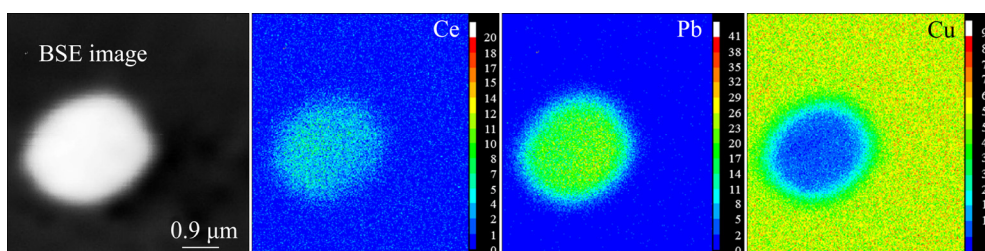


Fig. 3 Area distributions of elements with electron probe microanalysis (EPMA) for second phase

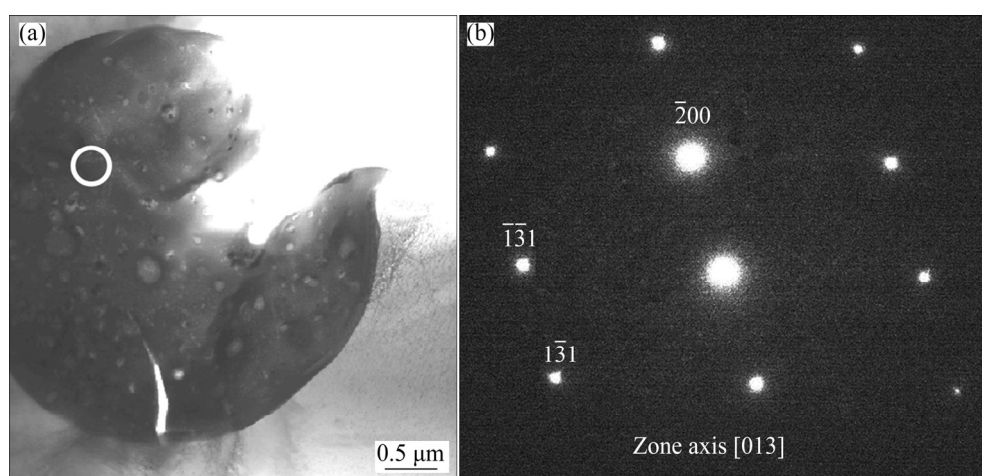


Fig. 4 TEM image (a) and selected area electron diffraction pattern (b) of second phase in Cu-0.1Pb-0.3Ce

copper, and the average columnar crystal spacing of Cu-0.1Pb is approximately 306.9 μm (Fig. 5(b)). Cu-0.1Pb-0.3Ce has small equiaxed grains, with

a size of ~137.1 μm, which shows that Ce addition has an obvious refining effect on the grain size (Fig. 5(c)).

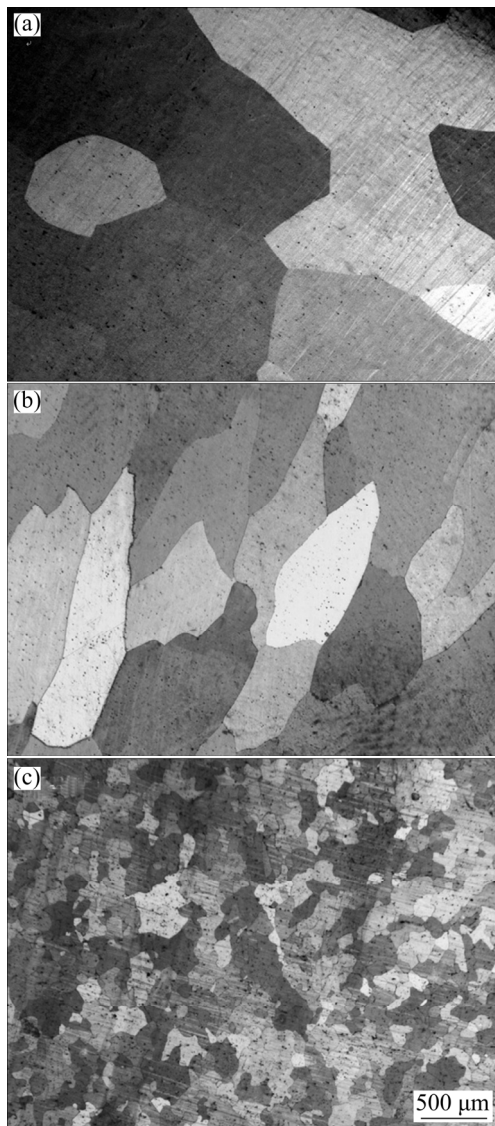


Fig. 5 Optical micrographs of impure copper containing Pb before and after Ce addition: (a) Pure copper; (b) Cu-0.1Pb; (c) Cu-0.1Pb-0.3Ce

Pb has a lower melting point (327.6 °C) than Cu. Pb agglomerates into the front of the liquid phase of the solid-liquid interface during solidification process. As a consequence, the degree of constitutional undercooling and the driving force of nucleation are increased, and the grain size of Cu-0.1Pb is refined. Ce addition leads to the formation of CePb₃. CePb₃ particles as heterogeneous nucleation centers refine the grain size of Cu-0.1Pb-0.3Ce. According to the theory of heterogeneous nucleation [28,29], two factors affect the second phase induced heterogeneous nucleation. One factor is that the melting point of the second phase is higher than that of the matrix. CePb₃ phase has a higher melting point than Cu. The other factor

is that the lattice misfit between the second phase and the matrix is less than 6%. The calculation equation of the lattice misfit between CePb₃ and Cu is as follows [30,31]:

$$\delta_{(hkl)_{\text{Cu}}^{(hkl)_{\text{CePb}_3}} = \frac{|d[uvw]_{\text{CePb}_3} \cdot \cos \theta - d[uvw]_{\text{Cu}}|}{d[uvw]_{\text{Cu}}} \times 100\% \quad (1)$$

where δ is the lattice misfit; $(hkl)_{\text{CePb}_3}$ and $(hkl)_{\text{Cu}}$ are the low-index surfaces of CePb₃ and Cu, respectively; $[uvw]_{\text{CePb}_3}$ and $[uvw]_{\text{Cu}}$ are the low-index orientations of CePb₃ and Cu, respectively; $d[uvw]_{\text{CePb}_3}$ and $d[uvw]_{\text{Cu}}$ are the atomic distances of the low-index orientations of CePb₃ and Cu, respectively; θ is the angle of the low-index orientations between CePb₃ and Cu. Figure 6 shows the misfitting relationship between (100) of Cu and (110) of CePb₃. The value of $d(100)_{\text{Cu}}$ is 0.3615 nm and the value of $d(110)_{\text{CePb}_3}$ is about 0.3448 nm [32]. θ value between $[1/2 \ 1/2 \ 0]$ orientation of CePb₃ and $[100]$ orientation of Cu is 0°. Therefore, the misfit between $[1/2 \ 1/2 \ 0]$ orientation of CePb₃ and $[100]$ orientation of Cu is ~4.62%, which agrees well with the previous experimental results [18,33]. CePb₃ second phase particles can act as effective heterogeneous nucleation centers and refine the grain size.

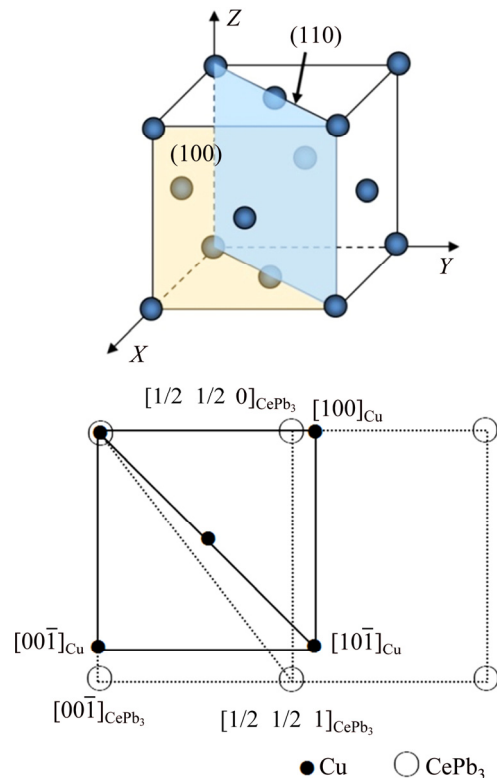


Fig. 6 Misfitting relationship between (100) of Cu and (110) of CePb₃

3.3 Effects of Ce on mechanical properties of impure copper containing Pb

Figure 7 shows the effects of Ce on the mechanical properties of impure copper containing Pb. The existence of Pb deteriorates the mechanical properties of copper remarkably. Compared to pure copper, the tensile strength and the elongation of Cu–0.1Pb are about 82.5 MPa and 15.3%, which are reduced by 43.1% and 56.7%, respectively. Ce addition improves the mechanical properties of impure copper containing Pb. Compared to Cu–0.1Pb, the tensile strength and the elongation of

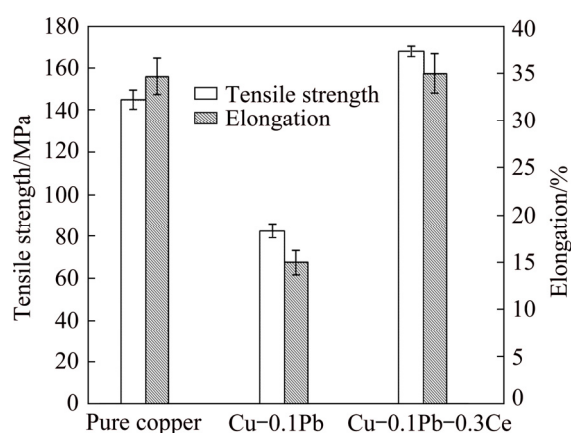


Fig. 7 Effects of Ce on mechanical properties of impure copper containing Pb

Cu–0.1Pb–0.3Ce are 179.5 MPa and 38.5%, which are increased by 117.6% and 151.6%, respectively. The mechanical properties of Cu–0.1Pb–0.3Ce are even a little better than those of pure copper.

The segregation of impurity element Pb at grain boundaries increases the inhomogeneity of chemical compositions and decreases the binding force of grain boundaries. Grain boundaries are the stress concentration zones during the tensile testing and cracks would be initiated on grain boundaries [34]. Hence, the mechanical properties of impure copper containing Pb are deteriorated. Ce addition purifies the grain boundaries, decreases the content of Pb on grain boundaries and changes the existence form of Pb by forming CePb_3 second phase particles. The second-phase strengthening improves the mechanical properties of impure copper containing Pb. On the other hand, as can be seen from Fig. 5, Ce addition refines the grain size. The fine-grain strengthening is also beneficial to the improvement of mechanical properties [35,36].

Figure 8 shows the SEM fractographs of impure copper containing Pb before and after Ce addition. Some deep and homogeneous dimples exist on the fracture surface of pure copper (Fig. 8(a)), showing good ductility. There are shallow and large dimples on the fracture surface of

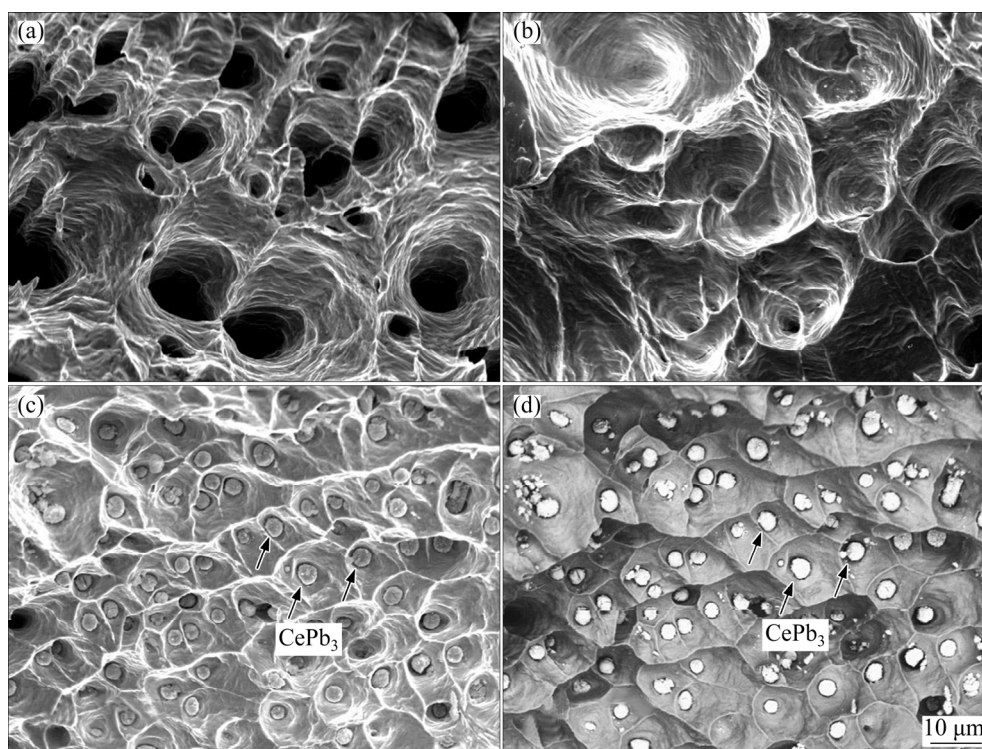


Fig. 8 SEM fractographs of impure copper containing Pb before and after Ce addition: (a) Pure copper; (b) Cu–0.1Pb; (c) Cu–0.1Pb–0.3Ce; (d) Backscattered electron image of Cu–0.1Pb–0.3Ce

Cu–0.1Pb (Fig. 8(b)), indicating the worse mechanical property than pure copper. As shown in Figs. 8(c, d), a large number of small dimples distribute uniformly on the fracture surface of Cu–0.1Pb–0.3Ce. Some spherical particles with average size of 3.1 μm are presented in the dimples. These second phase particles increase the resistance of resisting plastic deformation [37,38], which improves the mechanical properties of impure copper containing Pb. The fractographs of impure copper containing Pb before and after Ce addition are in well consistent with the variation rules of the mechanical properties.

4 Conclusions

(1) The minor amount of impurity element Pb mainly distributes on grain boundaries of copper, which can lower the binding force of grain boundaries. The tensile strength and the elongation of Cu–0.1Pb are decreased by 43.1% and 56.7% compared with those of pure copper, respectively.

(2) The Pb distributes from mainly at grain boundaries to homogeneously in the copper matrix with spherical particles after Ce addition. TEM combined with EDS results demonstrates that the structure of second phase particle is CePb_3 with AuCu_3 -type fcc structure.

(3) Due to the fine-grain strengthening and CePb_3 second-phase strengthening, Ce addition improves the mechanical properties of Cu–0.1Pb. Compared to Cu–0.1Pb, the tensile strength and the elongation of Cu–0.1Pb–0.3Ce are 179.5 MPa and 38.5%, which are increased by 117.6% and 151.6%, respectively.

References

- [1] CHEN Jing-jing, WANG Zhao-hui, WU Yu-feng, LI Li-quan, LI Bin, PAN De-an, ZUO Tie-yong. Environmental benefits of secondary copper from primary copper based on life cycle assessment in China [J]. *Resources Conservation and Recycling*, 2019, 146: 35–44.
- [2] LI Hai-hong, ZHANG Shi-hong, CHEN Yan, CHENG Ming, SONG Hong-wu, LIU Jin-song. Microstructure and properties of impure red-coppers refined by rare earths [J]. *Chinese Journal of Rare Metals*, 2016, 40: 48–55. (in Chinese)
- [3] CAMURRI C, CARRASCO C, LEITE R, MANGALARAJA R, DILLE J. Influence of impurities in cathodic copper on the ductility of copper wires [J]. *Journal of Materials Engineering and Performance*, 2012, 21: 1474–1478.
- [4] OTTO F, VISWANATHAN G B, PAYTON E J, FRENZEL J, EGgeler G. On the effect of grain boundary segregation on creep and creep rupture [J]. *Acta Materialia*, 2012, 60: 2982–2998.
- [5] GOODWIN L, NEEDS R J, HEINE V. Effect of impurity bonding on grain-boundary embrittlement [J]. *Physical Review Letters*, 1988, 60: 2050–2053.
- [6] DUSHER G, CHISHOLM M F, ALBER U, RUHLE M. Bismuth-induced embrittlement of copper grain boundaries [J]. *Nature Materials*, 2004, 3: 621–266.
- [7] ARMSTRONG D E J, WILKINSON A J, ROBERTS S G. Micro-mechanical measurements of fracture toughness of bismuth embrittled copper grain boundaries [J]. *Philosophical Magazine Letters*, 2012, 91: 394–400.
- [8] YAGODZINSKY Y, MALITCKII E, SAUKKONEN T, HÄNNINEN H. Hydrogen-enhanced creep and cracking of oxygen-free phosphorus-doped copper [J]. *Scripta Materialia*, 2012, 67: 931–934.
- [9] TAO Xiao-ma, WANG Zi-ru, LAN Chun-xiang, XU Guang-long, OUYANG Yi-fang, DU Yong. Exploring phase stability, electronic and mechanical properties of Ce–Pb intermetallic compounds using first-principles calculations [J]. *Journal of Solid State Chemistry*, 2016, 237: 385–393.
- [10] LI Hai-hong, ZHANG Shi-hong, CHEN Yan, CHENG Ming, SONG Hong-wu, LIU Jin-song. Effects of small amount addition of rare earth Ce on microstructure and properties of cast pure copper [J]. *Journal of Materials Engineering and Performance*, 2015, 24: 2857–2865.
- [11] ROSALBINO F, CARLINI R, SOGGIA F, ZANICCHI G, SCAVINO G. Influence of rare earth metals addition on the corrosion behaviour of copper in alkaline environment [J]. *Corrosion Science*, 2012, 58: 139–144.
- [12] CHEN Yan, ZHANG Shi-hong, SONG Hong-wu, CHENG Ming, LI Hai-hong, LIU Jin-song. Sudden transition from columnar to equiaxed grain of cast copper induced by rare earth microalloying [J]. *Materials and Design*, 2016, 91: 314–320.
- [13] LI Hai-yan, ZHOU Xuan, LU Xue-qiong, WANG Ya-ping. Effect of La on arc erosion behaviors and oxidation resistance of Cu alloys [J]. *Transactions of Nonferrous Metals Society of China*, 2017, 27: 102–109.
- [14] LIN Gao-yong, ZHOU Yu-xiong, ZENG Ju-hua, ZOU Yan-ming, LIU Jian, SUN Li-ping. Influence of rare earth elements on corrosion behavior of Al–brass in marine water [J]. *Journal of Rare Earths*, 2011, 29: 638–644.
- [15] DUAN Jun-wei, LIU Chu-ming. Choice of melting equipments of continuous casting and rolling process during the production of purple copper rods [J]. *Nonferrous Metals Processing*, 2011, 40: 22–24. (in Chinese)
- [16] CHEN Yan, CHENG Ming, SONG Hong-wu, ZHANG Shi-hong, ZHU Yan. Effects of lanthanum addition on microstructure and mechanical properties of as-cast pure copper [J]. *Journal of Rare Earths*, 2014, 32: 1056–1063.
- [17] ZHANG Zhen-feng, LIN Gao-yong, ZHANG Sheng-hua, ZHOU Jia. Effects of Ce on microstructure and mechanical properties of pure copper [J]. *Materials Science and Engineering A*, 2007, 457: 313–318.
- [18] LI Dao-yun, XU Lian-tang, FU Nian-xin, ZHAN Song-jiang. Study on rare earth to prevent segregation of high lead bronze [J]. *Journal of the Chinese Society of Rare Earths*, 1991, 9: 56–60. (in Chinese)

- [19] LI Ji-lin, CHANG Li-li, LI Sheng-li, ZHU Xin-de, AN Zhong-xin. Microstructure and properties of as-cast Cu–Cr–Zr alloys with lanthanum addition [J]. Journal of Rare Earths, 2018, 36: 424–429.
- [20] LI Wen-sheng, LIU Yi, WANG Zhi-ping, MA Chao, WANG Shun-cai. Effects of Ce in novel bronze and its plasma sprayed coating [J]. Transactions of Nonferrous Metals Society of China, 2012, 22: 2139–2145.
- [21] GUO F A, XIANG C J, YANG C X, CAO X M, MU S G, TANG Y Q. Study of rare earth elements on the physical and mechanical properties of a Cu–Fe–P–Cr alloy [J]. Materials Science and Engineering B, 2008, 147: 1–6.
- [22] LU Xi-li, CHEN Feng, LI, Wei-shu, ZHENG Yu-feng. Effect of Ce addition on the microstructure and damping properties of Cu–Al–Mn shape memory alloys [J]. Journal of Alloys and Compounds, 2009, 480: 608–611.
- [23] ZOU Jin, LU Lei, LU De-ping, LIU Ke-ming, CHEN Zhi-bao, ZHAI Qi-jie. Effect of boron and cerium on corrosion resistance of Cu–Fe–P alloy [J]. Journal of Materials Engineering and Performance, 2016, 25: 1062–1067.
- [24] LIN Gao-yong, LI Kun, FENG Di, FENG Yong-ping, SONG Wei-yuan, XIAO Meng-qiong. Effects of La–Ce addition on microstructure and mechanical properties of Al–18Si–4Cu–0.5Mg alloy [J]. Transactions of Nonferrous Metals Society of China, 2019, 29: 1592–1600.
- [25] ZHANG Cheng, JIANG Wen-long, YANG Bin, LIU Da-chun, Xu Bao-qiang, Yang Hong-wei. Experimental investigation and calculation of vapor–liquid equilibria for Cu–Pb binary alloy in vacuum distillation [J]. Fluid Phase Equilibria, 2015, 405: 68–72.
- [26] ZHAO Jiu-zhou, AHMED T, JIANG Hong-xiang, HE Jie, SUN Qian. Solidification of immiscible alloys: A review [J]. Acta Metallurgica Sinica (English Letters), 2017, 30: 1–28.
- [27] GULAY L D. Investigation of the phase diagrams of the La–Cu–Pb and Ce–Cu–Pb systems [J]. Journal of Alloys and Compounds, 2002, 347: 124–127.
- [28] CHO D H, NAM J H, LEE B W, CHO K M, PARK I M. Effect of Mn addition on grain refinement of biodegradable Mg4Zn0.5Ca alloy [J]. Journal of Alloys and Compounds, 2016, 676: 461–468.
- [29] YANG Wen-chao, LIU Lin, ZHANG Jun, JI Shou-xun, FAN Zhong-yun. Heterogeneous nucleation in Mg–Zr alloy under die casting condition [J]. Materials Letters, 2015, 160: 263–267.
- [30] BRAMFITT B L. Planar lattice disregistry theory and its application on heterogistry nuclei of metal [J]. Metallurgical and Materials Transactions A, 1970, 1: 1987–1995.
- [31] LIU Zheng, CHEN Qing-chun, GUO Song, LIU Jun-yi, HU Qian-qian. Calculation of planar disregistries between compounds of rare earth–Al and primary α phase in A356–RE alloy and its verification [J]. Rare Metal Materials and Engineering, 2015, 44: 859–865. (in Chinese)
- [32] WYCKOFF R W G. crystal structures [M]. 2nd ed. New York: Interscience Publishers, 1963.
- [33] TAN Rong-sheng, GUO Fang, SUN Lian-chao. Phase identification of rare earth phases in deformed high lead brass [J]. Journal of the Chinese Society of Rare Earths, 1991, 9: 181–182. (in Chinese)
- [34] LU L, CHEN X, HUANG X, LU K. Revealing the maximum strength in nanotwinned copper [J]. Science, 2009, 323: 607–610.
- [35] JIANG X, SONG S H. Enhanced hot ductility of a Cr–Mo low alloy steel by rare earth cerium [J]. Materials Science and Engineering A, 2014, 613: 171–177.
- [36] LI M Z, WANG Y Q, LI C, LIU X G, XU B S. Effects of neodymium rich rare earth elements on microstructure and mechanical properties of as cast AZ31 magnesium alloy [J]. Materials Science and Technology, 2011, 27: 1138–1142.
- [37] GOLMAKANIYOON S, MAHMUDI R. Microstructure and creep behavior of the rare-earth doped Mg–6Zn–3Cu cast alloy [J]. Materials Science and Engineering A, 2011, 528: 1668–1677.
- [38] CHEN Zhong-wei, CHEN Pei, MA Cui-ying. Microstructures and mechanical properties of Al–Cu–Mn alloy with La and Sm addition [J]. Rare Metals, 2012, 31(4): 332–335.

稀土铈对含铅杂铜显微组织和力学性能的影响

李海红¹, 刘晓¹, 李杨¹, 张士宏², 陈岩², 王松伟², 刘劲松², 吴金虎³

1. 烟台大学 核装备与核工程学院, 烟台 264005;

2. 中国科学院 金属研究所, 沈阳 110016; 3. 华北理工大学 冶金与能源学院, 唐山 063210

摘 要: 采用光学显微镜、扫描电镜、电子探针、透射电镜和拉伸实验研究稀土 Ce 对含 Pb 杂铜显微组织和力学性能的影响。透射电镜和能谱分析表明, Ce 与 Pb 形成球状 CePb₃ 颗粒, 粒径约 3.6 μm , 均匀分布在铜基体中。CePb₃ 与铜基体的错配度较低(约 4.62%), 可以作为有效成核质点, 有利于晶粒细化。Pb 存在于晶界会恶化铜的力学性能, Cu–0.1Pb 的抗拉强度和伸长率分别比纯铜降低 43.1% 和 56.7%。Ce 加入能净化铜的晶界, 形成 CePb₃ 第二相颗粒, 细化晶粒尺寸, 提高铜的力学性能。与 Cu–0.1Pb 相比, Cu–0.1Pb–0.3Ce 的抗拉强度(179MPa)和伸长率(38.5%)分别提高 117.6%和 151.6%。

关键词: Ce 添加; 含 Pb 杂铜; CePb₃ 第二相颗粒; 晶格错配度; 晶粒细化; 力学性能

(Edited by Bing YANG)